# SLIDING MODE CONTROL

## INTRODUCTION

### Overview of MIMO sliding mode control

The controller design starts with a standard linear state space representation:

$$\dot{x} = Ax + Bu \tag{120}$$

where:

$A \in \Re^{mxm}$, state matrix

$B \in \Re^{mxn}$, control matrix

$x \in \Re^{mx1}$, state vector

$u \in \Re^{nx1}$, control vector

The sliding mode control law, *u*, is composed of two main parts:

$$u = \hat{u} + \bar{u} \tag{121}$$

The first part, $\hat{u}$, is a linear feedback based on the linear representation given by Equation (120). The second part, $\bar{u}$, are nonlinear feedbacks with their signs switching depending on the relationship of the system states to the sliding surfaces. The sliding surfaces are hyper planes in the state space, with one for each control. They are defined by:

$$\sigma(x) = S^T x = 0 \tag{122}$$

Where:

$$S \in \Re^{nxm}$$

To determine the nonlinear feedback functions, the concept of Liapunov stability is used. The Liapunov function is taken as:

$$V(x) = \frac{1}{2}\left(\sigma_1^2 + \sigma_2^2 + \ldots + \sigma_n^2\right) \tag{123}$$

Asymptotic system stability is guaranteed provided that $\dot{V}(x)$ is a positive definite function, that is:

$$\dot{V}(x) = \dot{\sigma}_1\sigma_1 + \dot{\sigma}_2\sigma_2 + \ldots + \dot{\sigma}_n\sigma_n < 0 \tag{124}$$

Equation (124) is satisfied if:

$$\dot{\sigma}_i\sigma_i < 0 \text{ for } i = 1 \text{ to } n \tag{125}$$

Equation (125) can be rewritten as:

$$\dot{\sigma}_i = -\eta_i sign(\sigma_i) \tag{126}$$

where $\eta_i$ is a positive gain parameter for the $i^{th}$ sliding surface. Equation (126) can be rewritten after substituting the time derivative of Equation (122) and Equation (120) as:

$$S^T(Ax + Bu) = -\begin{bmatrix} \eta_1 sign(\sigma_1) \\ \eta_2 sign(\sigma_2) \\ . \\ . \\ . \\ \eta_n sign(\sigma_n) \end{bmatrix} \tag{127}$$

Solving Equation (127) for $u$ yields:

$$u = -(S^T B)^{-1} S^T Ax - (S^T B)^{-1} \begin{bmatrix} \eta_1 sign(\sigma_1) \\ \eta_2 sign(\sigma_2) \\ . \\ . \\ . \\ \eta_n sign(\sigma_n) \end{bmatrix} \tag{128}$$

Equation (128) can be rewritten in matrix form as:

$$u = Kx + K_s \eta sign(\sigma) \tag{129}$$

where:

$$K = -(S^T B)^{-1} S^T A$$

$$K_s = -(S^T B)^{-1}$$

Equation (129) is identical in form to Equation (121), with a linear state feedback and a nonlinear switching term.

For the decomposition in Equation (128), it is required that the closed loop stability matrix, (*A-BK*), have *n* zero eigenvalues. The sliding surfaces are the left eigenvectors resulting from the zero eigenvalues.

**Utkin's method for MIMO sliding mode control law design**

Determination of the sliding surfaces can be difficult, especially with a MIMO system. One technique for this is proposed by Utkin (1977). For this technique to be applied, the B matrix of the state space system (Equation (120)) must be of the form:

$$B = \begin{bmatrix} B_1 \\ 0 \end{bmatrix} \tag{130}$$

where:

$$B_1 \in \Re^{nxn}$$

$$0 \in \Re^{(m-n)xn}$$

For the MIMO cases of vertical plane depth control used in this thesis, this was the case. For the stern planes only control examples, a QR factorization was applied, to transform the state space system into this form.

Given that the B matrix is of the form defined in Equation (130), Equation (120) can be decomposed into the following:

$$x_1 = A_{11} x_1 + A_{12} x_2 + B_1 u \tag{131}$$

$$x_2 = A_{21}x_1 + A_{22}x_2 \tag{132}$$

where:

$$x_1 \in \Re^{nx1}$$

$$x_2 \in \Re^{(m-n)x1}$$

$$A_{11} \in \Re^{nxn}$$

$$A_{12} \in \Re^{nx(m-n)}$$

$$A_{21} \in \Re^{(m-n)xn}$$

$$A_{22} \in \Re^{(m-n)x(m-n)}$$

The sliding surfaces become:

$$\sigma = S_1^T x_1 + S_2^T x_2 = 0 \tag{133}$$

where:

$$S_1^T \in \Re^{nxn}$$

$$S_2^T \in \Re^{nx(m-n)}$$

Because the sliding surfaces are the left eigenvectors of the *n* zero eigenvalues, $S_1^T$ can be set to the identity matrix without loss of generality. Substitution of Equation (133) into Equation (148) leads to:

$$\dot{\sigma} = \dot{x}_1 + S_2^T \dot{x}_2 = -\eta sign(x_1 + S_2^T x_2) \tag{134}$$

$$u = -B_1^{-1}\left[(A_{11} + S_2^T A_{21})x_1 + (A_{12} + S_2^T A_{22})x_2\right] - B_1^{-1}\begin{bmatrix} \eta_1 sign(\sigma_1) \\ \eta_2 sign(\sigma_2) \\ . \\ . \\ . \\ \eta_n sign(\sigma_n) \end{bmatrix} \tag{135}$$

When the system is on the sliding surfaces, Equation (133) can be used to solve for $x_1$ in terms of $x_2$, resulting in:

$$x_1 = -S_2^T x_2 \tag{136}$$

Substitution of this result into Equation (132) results in:

$$\dot{x}_2 = (A_{22} - A_{21}S_2^T)x_2 \tag{137}$$

Equation (137) is the set of independent equations that the non zero eigenvalues for the control result from. For the application of pole placement algorithms to determine the sliding surfaces, it only has to be recognized that it is in the standard state space format:

$$\dot{y} = \hat{A}y + \hat{B}\hat{K}y \tag{138}$$

with:

$$\hat{A} = A_{22}$$

$$\hat{B} = -A_{21}$$

$$\hat{K} = S_2^T$$

Once $S_2^T$ is determined, the control law can be determined by substituting it into Equation (135).

Utkin's technique also allows for the use of linear quadratic regulator methods for determination of the sliding surfaces. (Utkin 1977) For this method, it is desired to minimize a quadratic performance index:

$$I = \frac{1}{2}\int_0^\infty x^T Q x dt \tag{139}$$

where $Q$ is a positive definite weighting matrix. By partitioning $Q$ in the same manner as $A$ was partitioned for equations (131)and (132), Equation (139) can be rewritten as:

$$I = \frac{1}{2}\int_0^\infty (x_1{}^T Q_{11} x_1 + x_2{}^T Q_{21} x_1 + x_1{}^T Q_{12} x_2 + x_2{}^T Q_{22} x_2) dt \tag{140}$$

or:

$$I = \frac{1}{2}\int_0^\infty (x_2{}^T Q^* x_2 + v^T Q_{11} v^T) dt \tag{141}$$

where:

$$Q^* = Q_{22} - Q_{21} Q_{11}^{-1} Q_{12}$$

$$A^* = A_{22} - A_{21} Q_{11}^{-1} Q_{12}$$

$$v = x_1 + Q_{11}^{-1} Q_{12} x_1$$

With the system on the sliding surfaces, Equation (140) can be rewritten as:

$$\dot{x}_2 = A^* x_2 + A_{21} v \tag{142}$$

Equations (141) and (142) are in a recognizable form for the application of any convenient linear quadratic regulator solution. The Hamiltonian is:

$$H = p^T(A^* x_2 + A_{21}v) - \frac{1}{2}(x_2^T Q^* x_2 + v^T Q_{11} v) \tag{143}$$

The algebraic Riccati equation is:

$$(A^*)^T k + kA^* - kA_{21}Q_{11}^{-1}A_{21}^T k + Q^* = 0 \tag{144}$$

The solution of Equation (144) results in:

$$v = -Q_{11}^{-1}A_{21}^T k x_2 \tag{145}$$

This result is used with the definition for $v$ from Equation (141) to provide the relationship between $x_1$ and $x_2$. This results in the sliding surface:

$$S_2^T = Q_{11}^{-1}(Q_{12} + A_{21}^T k) \tag{146}$$

With $S_2^T$ determined, the control law can be determined by substitution into Equation (135).

This sliding mode LQR controller design was implemented in a MATLAB® function SMLQR.M which included provisions for a QR factorization for the cases when the $B$ matrix was not of the form given by Equation (130). SMLQR.M is included in Appendix A.

**Control of chatter**

One undesirable aspect of sliding mode control is the chatter induced by the nonlinear switching term near the sliding surfaces. The nonlinear switching term in the sliding mode control can cause control chatter when the system is near a sliding surface. One way to reduce the chatter is to use the concept of a boundary layer around the sliding surface. First, a *satsign* function is defined:

$$satsign(x) = \begin{cases} 1, x > 1 \\ x, -1 \le x \le 1 \\ -1, x < -1 \end{cases} \tag{147}$$

A boundary layer of thickness $\phi$ around each sliding surface, is applied using the *satsign* function:

$$\dot{\sigma}_i = satsign\left(\frac{\sigma_i}{\phi_i}\right) \tag{148}$$

Equation (147) can be used to replace the *sign* function used in Equation (129) with no change

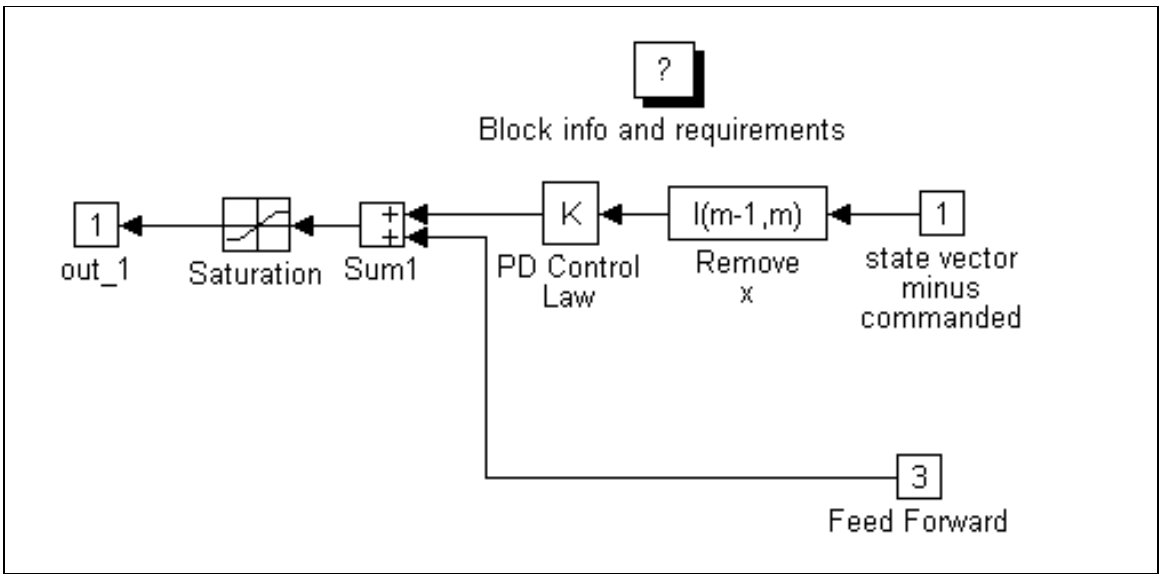


Figure 27. SIMULINK® model sliding mode controller

in the asymptotic stability of the system. There are some effects, however, because the dynamics near the sliding surface are not the same as the closed loop dynamics which exist when the system is on the sliding surface. The final control law is:

$$u = Kx + K_s \eta satsign\left(\frac{\sigma}{\phi}\right) \tag{149}$$

Equation (149) was implemented as a SIMULINK® model, shown in Figure 27.

## SIMO SLIDING MODE CONTROL RESPONSE TO DISTURBANCES

When applied to vertical plane submarine control, sliding mode control has several nuances which are not obvious from inspection of the governing equations. In order to illustrate these, the performance of sliding mode control will be explored through several example cases. To keep the analytic derivations simple, the cases worked will be done with stern planes control only. The general concepts, however, will be applicable to stern and bow planes control.

The response of sliding mode control to force and moment disturbances is fundamental to its application to submarine control in the vertical plane. These force and moment disturbances could result from a variety of situations. Examples of these include out of trim conditions, free surface effects, and wave forces.

### Basic sliding mode disturbance response

The first case will use a basic sliding mode control law, that is one without a feedforward term or integral control. The resulting control law is:

$$\sigma = S_1 w + S_2 q + S_3 \theta + S_4 \ z \tag{150}$$

$$\delta = K_1 w + K_2 q + K_3 \theta + \eta K_s satsign(\frac{\sigma}{\phi}) \tag{151}$$

$$|\delta| \le \delta_{\max} \tag{152}$$

#### *Linear analysis steady state*

Assuming that the sliding mode control is not saturated and that the control deflection is less than the maximum, the submarine should reach an equilibrium state under the action of steady force and or moment disturbances. The linear equations of motion in the vertical plane with one control are:

$$\dot{w} = a_{11} uw + a_{12} uq + a_{13} \theta + b_1 u^2 \delta \ + F_d \tag{153}$$

$$\dot{q} = a_{21} uw + a_{22} uq + a_{23} \theta + b_2 u^2 \delta + M_d \tag{154}$$

$$\dot{\theta} = q \tag{155}$$

$$\dot{z} = w - u\theta \tag{156}$$

$$\dot{x} = w\theta + u \tag{157}$$

Equations (150) through (157) can be solved for the following steady state condition:

$$w_{ss} = \frac{F_d(-ub_2) + M_d(ub_1)}{b_2 a_{11} u^2 + b_2 a_{13} - b_1 a_{21} u^2 - b_1 a_{23}} \tag{158}$$

$$q_{ss} = 0 \tag{159}$$

$$\theta_{ss} = \frac{F_d(-b_2) + M_d(b_1)}{b_2 a_{11} u^2 + b_2 a_{13} - b_1 a_{21} u^2 - b_1 a_{23}} \tag{160}$$

$$\begin{aligned} z_{ss} = F_d & \frac{a_{21}u^2 + K_3 u^2 b_2 + a_{23} + u^3 \eta K_s \phi b_2 S_1 + u^2 \eta K_s \phi b_2 S_3 + K_1 u^3 b_2}{u^2 K_n S_4 \phi (b_2 a_{11} u^2 + b_2 a_{13} - b_1 a_{21} u^2 - b_1 a_{23})} \\ - M_d & \frac{K_3 u^2 b_1 + a_{11} u^2 + a_{13} + u^3 \eta K_s \phi b_1 S_1 + K_1 u^3 b_1 + u^2 \eta K_s \phi b_1 S_3}{u^2 K_n S_4 \phi (b_2 a_{11} u^2 + b_2 a_{13} - b_1 a_{21} u^2 - b_1 a_{23})} \end{aligned} \tag{161}$$

$$\delta_{ss} = \frac{F_d(a_{21}u^2 + a_{23}) + M_d(-a_{11}u^2 - a_{13})}{u^2(b_2 a_{11} u^2 + b_2 a_{13} - b_1 a_{21} u^2 - b_1 a_{23})} \tag{162}$$

If the sliding mode is just saturated, that is $|\sigma / \phi| = 1$, the system will still be stable, however the gain parameter $\eta$ will be at a critical value. If further reduced, the system will be unstable. Assuming the sliding mode is just saturated this critical value, $\eta_{crit}$, can be determined.

$$\eta_{crit} = \left| \begin{aligned} & F_d \frac{a_{21}u^2 + a_{23} + K_3 u^2 b_2 + K_1 u^3 b_2}{K_s u^2 (b_2 a_{11} u^2 + b_2 a_{13} - b_1 a_{21} u^2 - b_1 a_{23})} \\ & - M_d \frac{a_{11}u^2 + a_{13} + K_3 u^2 b_1 + K_1 u^3 b_1}{K_s u^2 (b_2 a_{11} u^2 + b_2 a_{13} - b_1 a_{21} u^2 - b_1 a_{23})} \end{aligned} \right| \tag{163}$$

For cases with the gain parameter $\eta$ less than critical, a steady state $\dot{z}$ results, along with steady state values in all states other than $z$. By assuming a steady state $\dot{z}$ and solving Equations (150) through (157) for equilibrium, the following equations result:

$$\theta_{ss} = \frac{F_d(-a_{21} - b_2 u K_1) + Md(b_1 u K_1 + a_{11}) + u^2 K_s \eta (b_2 a_{11} - b_1 a_{21})}{u^2 K_3 (b_1 a_{21} - b_2 a_{11}) + u K_1 (a_{13} b_2 - a_{23} b_1) + a_{13} a_{21} - a_{23} a_{11}} \tag{164}$$

$$\dot{z}_{ss} = -\frac{F_d + b_1 u^2 K_s \eta + \theta_{ss}(a_{13} + a_{11} u^2 + b_1 u^3 K_1 + b_1 u^2 K_3)}{u(b_1 u K_1 + a_{11})} \tag{165}$$

$$w_{ss} = u\theta_{ss} + \dot{z}_{ss} \tag{166}$$

$$q_{ss} = 0 \tag{167}$$

$$\delta_{ss} = \frac{-(a_{11} u w_{ss} + a_{13}\theta_{ss} + F_d)}{b_1 u^2} \tag{168}$$

Inspection of Equation (164) may cause the reader to incorrectly assume that a nonzero steady state value of $\theta$ will exist in the absence of disturbances. This is not the case, however, because the use of Equation (164) implies the lack of a steady state $z$, and therefore a disturbance.

***Nonlinear analysis steady state***

An analysis similar to that conducted on the linear equations can be conducted to determine the system steady state response under a constant disturbance. The nonlinear equations of motion in the vertical plane with one control are:

$$\dot{w} = a_{11} u w + a_{12} u q + a_{13} \sin(\theta) + b_1 u^2 \delta + F_d \cos(\theta) + e_{11} q^2 + e_{12} q w \tag{169}$$

$$\dot{q} = a_{21} u w + a_{22} u q + a_{23} \sin(\theta) + b_2 u^2 \delta + M_d \cos(\theta) + e_{21} q^2 + e_{22} q w \tag{170}$$

$$\dot{\theta} = q \tag{171}$$

$$\dot{z} = w\cos(\theta) - u\sin(\theta) \tag{172}$$

$$\dot{x} = w\sin(\theta) + u\cos(\theta) \tag{173}$$

Once again, the basic sliding mode control of Equations (150) and (151) is used. Assuming that steady state is possible (sliding mode control is not saturated, and the control deflection is less than the maximum) Equations (169) through (173) subject to the basic sliding mode control law can be reduced to the following nonlinear equation:

$$a_{11}\sin(\theta)u^2 b_2 + a_{13}\sin(\theta)\cos(\theta)b_2 + F_d\cos^2(\theta)b_2 - \\ b_1 a_{21}\sin(\theta)u^2 - b_1 a_{23}\sin(\theta)\cos(\theta) - b_1 M_d\cos^2(\theta) = 0 \tag{174}$$

Solution of Equation (174) yields the steady state value of $\theta$. It is of note that Equation (174) is independent of the control law. The correct root is readily determined by using the value closest to the linear analysis (Equation (160)). Substitution of this value into Equations (169) through (173) yields following steady state results:

$$w_{ss} = u\tan(\theta_{ss}) \tag{175}$$

$$q_{ss} = 0 \tag{176}$$

$$\delta_{ss} = \frac{-(a_{11}uw_{ss} + a_{13}\sin(\theta_{ss}) + F_d)}{b_1 u^2} \tag{177}$$

$$z_{ss} = \frac{\frac{\phi}{\eta K_s}(\delta_{ss} - K_1 w_{ss} - K_3\theta_{ss}) - S_1 w_{ss} - S_3\theta_{ss}}{S_4} \tag{178}$$

The steady state value of $z$ given by Equation (178) is dependent upon the control law gains. Following the example of the linear analysis, a critical value of the gain parameter, $\eta_{crit}$ can be determined.

$$\eta_{crit} = \left|\frac{\delta_{ss} - K_1 w_{ss} - K_3\theta_{ss}}{K_s}\right| \tag{179}$$

Unlike the linear analysis, the critical value of the gain parameter is not just a linear combination of the disturbance forces, but rather requires nonlinear solution for each possible case.

If $|\sigma/\phi| > 1$ the sliding mode control will be saturated, and a nonzero steady state $\dot{z}_{ss}$ will exist. For this case, the control law control law reduces to:

$$\delta = K_1 w + K_2 q + K_3 \theta + \eta K_s sign(\sigma) \tag{180}$$

Given the steady state final condition in all state variables with the exception of z, Equations (169) through (173) and (180) can be reduced to finding a root of the following nonlinear equation:

$$\frac{u^2(b_1K_3a_{21}\theta + b_1K_na_{21} - b_2K_3a_{11}\theta - b_2K_2a_{11}) + u\sin(\theta)(a_{13}b_2K_1 - a_{23}b_1K_1)}{b_2uK_1 + a_{21}} + \frac{F_d\cos(\theta)(b_2uK_1 + a_{21}) - M_d\cos(\theta)(b_1uK_1 + a_{11}) + \sin(\theta)(a_{13}a_{21} - a_{23}a_{11})}{b_2uK_1 + a_{21}} = 0 \tag{181}$$

This can be accomplished using the using the linear value of $\theta_{ss}$ from Equation (164) as the initial guess. It follows that:

$$\dot{z}_{ss} = -\frac{F_d\cos^2(\theta_{ss}) + a_{13}\sin(\theta_{ss})\cos(\theta_{ss})}{u(b_1uK_1 + a_{11})} - \frac{u^2(a_{11}\sin(\theta_{ss}) + b_1uK_1\sin(\theta_{ss}) + b_1K_3\theta_{ss}\cos(\theta_{ss}) + b_1K_s\eta\cos(\theta_{ss}))}{u(b_1uK_1 + a_{11})} \tag{182}$$

$$w_{ss} = u\tan(\theta_{ss}) + \dot{z}_{ss} \tag{183}$$

$$\delta_{ss} = K_1 w_{ss} + K_3\theta_{ss} + \eta K_s sign(\sigma) \tag{184}$$

***Disturbance response simulation with basic sliding mode***

These results can then be applied to the SUBOFF hydrodynamic coefficients. For the modified coefficients used in this thesis, the linear state space system at six knots with stern planes only is:

$$\begin{bmatrix} \dot{w} \\ \dot{q} \\ \dot{\theta} \\ \dot{z} \end{bmatrix} = \begin{bmatrix} -0.0179 & 3.7101 & 0.0196 & 0 \\ 0.0006 & -0.0680 & -0.0034 & 0 \\ 0 & 1 & 0 & 0 \\ 1 & 0 & -10.1269 & 0 \end{bmatrix} \begin{bmatrix} w \\ q \\ \theta \\ z \end{bmatrix} + \begin{bmatrix} -0.1009 \\ -.0027 \\ 0 \\ 0 \end{bmatrix} \delta + \begin{bmatrix} F_d \\ M_d \\ 0 \\ 0 \end{bmatrix} \tag{185}$$

A sliding mode control law is determined using Utkin's method. After some experimentation, the diagonal of the minimization matrix Q was selected as $Q_{11} = 100$, $Q_{22} = 100$, $Q_{33} = 100$, $Q_{44} = 1$. This yielded the following control law:

$$\sigma = 1.0w - 67.5592q - 15.4082\theta + 0.0830z \tag{186}$$

$$\delta = -0.2803w + 84.8572q + 7.0612\theta + K_s \eta satsign\left(\frac{\sigma}{\phi}\right) \tag{187}$$

$$|\delta| \leq 0.4 \tag{188}$$

A moment disturbance was chosen to be controllable but give a nontrivial response. The application of a force of five thousand pounds and moment of 4,573 thousand foot pounds resulted in a pure angular acceleration, $M_d = 0.001$ radians/second$^2$. For this state space system, control law, and disturbance set, the value of $\eta_{crit}$ was (0.0661). Application of the nonlinear solutions yielded the steady state solutions in Table 13.

| $\eta / \eta_{crit}$ | $w_{ss}(Feet/Sec)$ | $q_{ss}(Rad/\sec)$ | $\theta_{ss}(Degrees)$ | $z_{ss}(Feet)$ | $\delta_{ss}(Radians)$ | $\dot{z}_{ss}(Feet/Sec)$ |
|---|---|---|---|---|---|---|
| 0 | -0.9606 | 0 | -0.8271 | Infinity | 0.1673 | -0.8143 |
| 0.5 | -1.1791 | 0 | -4.3402 | Infinity | 0.1941 | -0.4094 |
| 1.1 | -1.3965 | 0 | -7.8518 | -19.5783 | 0.2208 | 0 |
| 2 | -1.3965 | 0 | -7.8518 | -14.6467 | 0.2208 | 0 |
| 4 | -1.3965 | 0 | -7.8518 | -11.6330 | 0.2208 | 0 |

Table 13. Steady state nonlinear solutions for $M_d = 0.001$ radians/second$^2$

The system transient response was simulated using the RK45 function of the SIMULINK® toolbox. Figure 28 shows the resulting paths. The response is given for six values of the ratio of $\eta$ and $\eta_{crit}$. As expected, for values of $\eta$ less than critical the control law is unable to maintain a steady depth.

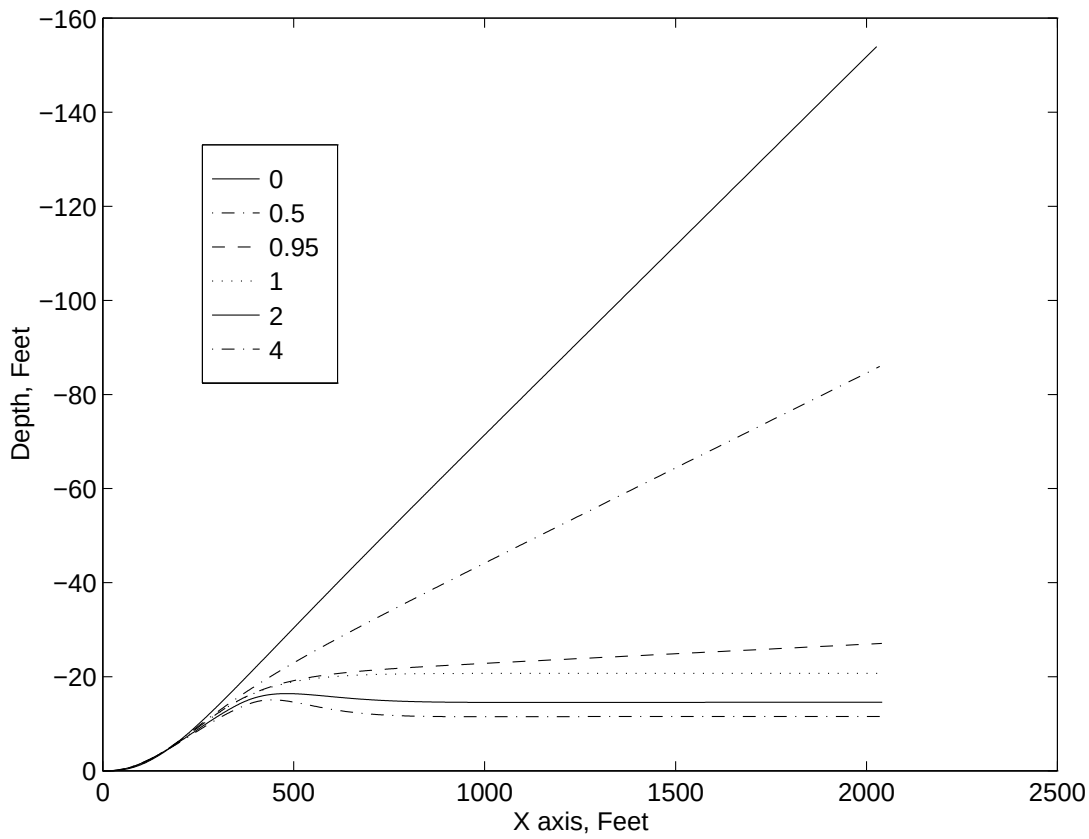


Figure 28. Nonlinear simulation of vertical plane response to a pure moment disturbance

The calculations and simulations were repeated for a pure force disturbance. A force of 43 thousand pounds and a moment of 220.4 foot thousand pounds resulted in a pure vertical acceleration of 0.005 feet/second$^2$. For this state space system, control law, and disturbance set, the value of $\eta_{crit}$ was (0.0466).

| $\eta / \eta_{crit}$ | $w_{ss}$ (*Feet / Sec*) | $q_{ss}$ (*Rad* / sec) | $\theta_{ss}$ (*Degrees*) | $z_{ss}$ (*Feet*) | $\delta_{ss}$ (*Radians*) | $\dot{z}_{ss}$ (*Feet / Sec*) |
|---|---|---|---|---|---|---|
| 0 | 1.5724 | 0 | 5.4888 | Infinity | 0.2357 | 0.5966 |
| 0.5 | 1.4156 | 0 | 2.9632 | Infinity | 0.2549 | 0.8902 |
| 1.1 | 1.8836 | 0 | 10.5368 | 22.4107 | 0.1976 | 0 |
| 2 | 1.8836 | 0 | 10.5368 | 17.4792 | 0.1976 | 0 |
| 4 | 1.8836 | 0 | 10.5368 | 14.4654 | 0.1976 | 0 |

Table 14. Steady state nonlinear solutions for $F_d = 0.05$

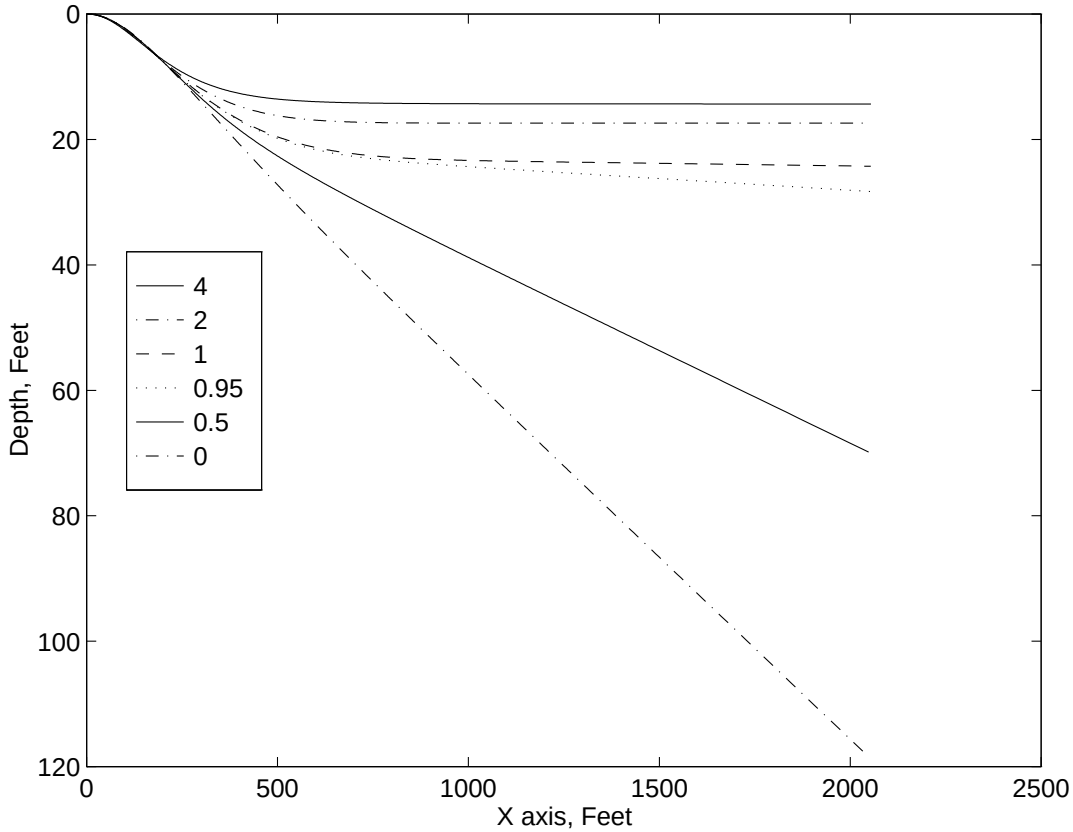


Figure 29. Nonlinear simulation of vertical plane response to a pure force disturbance

***Disturbance response with sliding mode feedforward control***

To eliminate the steady state error induced by a disturbance, several techniques may be employed. Using a feedforward function in the sliding mode control law is one technique. A feedforward term works by using knowledge of the external disturbance and using applying some degree of control effort. This provides a steady state control effort to oppose the disturbance without a steady state error. This approach is limited as it requires one control per zero error state and may be limited in other ways. A feedforward term can be added to the sliding mode control law by changing the sliding surface to the following:

$$\sigma = S_1 w + S_2 q + S_3 \theta + S_4 \ z + S_5 \tag{189}$$

The value of $S_5$ is such that it will equal the control effort that is applied by the steady state quantity that is desired to be zeroed. Since the main priority is to obtain zero

depth error, $S_5$ is selected to equal the control effort introduced by the previously calculated value of steady state depth error:

$$S_5 = \frac{\phi}{\eta K_s}(\delta_{ss} - K_1 w_{ss} - K_3 \theta_{ss}) - S_1 w_{ss} - S_3 \theta_{ss} \tag{190}$$

The steady state values needed for Equation (190) can be determined from linear or nonlinear analysis, although the linear analysis will result in a non-zero depth error. The linear analysis gives the following:

$$S_5 = C_1 M_d + C_2 F_d \tag{191}$$

where:

$$C_1 = \frac{-\left(\frac{\phi}{S_4 K_s \eta}\left(a_{11} + \frac{a_{13}}{u^2} + K_3 b_1 + K_1 u b_1\right) + \frac{S_3 b_1}{S_4} + \frac{S_1 u b_1}{S_4}\right)}{a_{11} u^2 b_2 + a_{13} b_2 - b_1 a_{21} u^2 - b_1 a_{23}} \tag{192}$$

$$C_2 = \frac{\left(\frac{\phi}{S_4 K_s \eta}\left(a_{21} + \frac{a_{23}}{u^2} + K_3 b_2 + K_1 u b_2\right) + \frac{S_3 b_2}{S_4} + \frac{S_1 u b_2}{S_4}\right)}{a_{11} u^2 b_2 + a_{13} b_2 - b_1 a_{21} u^2 - b_1 a_{23}} \tag{193}$$

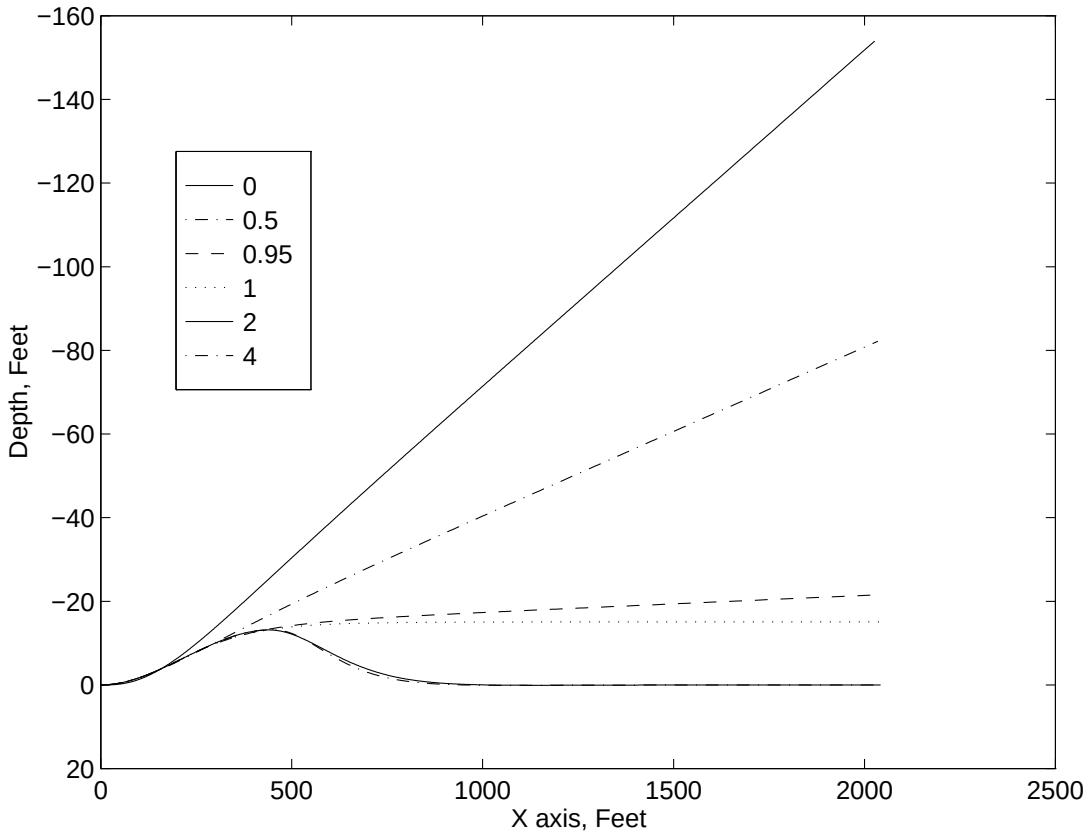


Figure 30. Nonlinear simulation of vertical plane response to a pure moment disturbance with a feedforward term based on nonlinear steady state

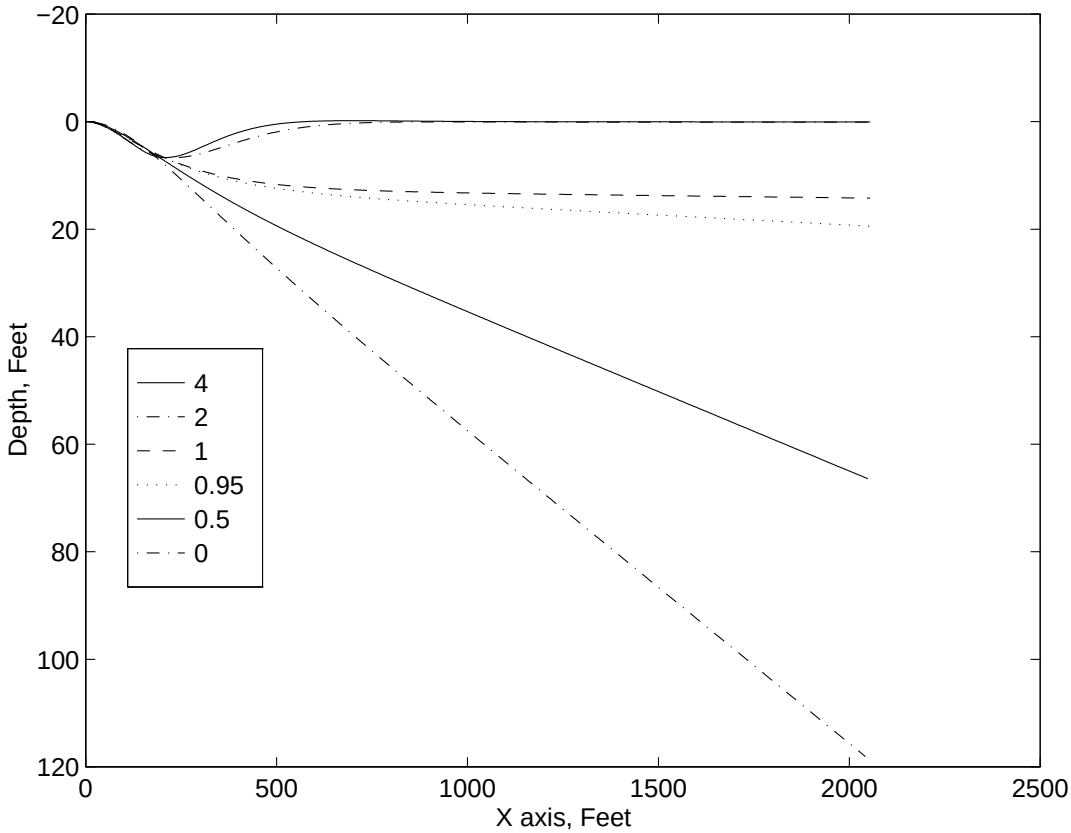


Figure 31. Nonlinear simulation of vertical plane response to a pure force disturbance with a feedforward term based on nonlinear steady state

***Disturbance response with sliding mode integral control***

Another means of eliminating steady state error is by the use of an integral control term. To accomplish this, an additional equation is added to the state space representation.

$$\dot{z}_I = z \tag{194}$$

This forces a zero steady state error in $z$, although there are some additional considerations with the use of integral control. The resulting control law, with the additional state, is:

$$\sigma = S_1 w + S_2 q + S_3 \theta + S_4 \ z + S_5 z_I \tag{195}$$

$$\delta = K_1 w + K_2 q + K_3 \theta + K_4 z + \eta K_s satsign(\frac{\sigma}{\phi}) \tag{196}$$

$$|\delta| \leq 0.4 \tag{197}$$

Based on inspection of Equations (195) and (196) several conclusions can be drawn. First, because $z$ is included in the proportional portion of the control law, values of the gain parameter which are less than critical will result in a steady state error in $z$ for any controllable disturbance. Second, if there is a steady state error in $z$, the magnitude of the integral term, $z_I$, will tend to infinity. This can cause problems with changing conditions or pathkeeping as it will delay the control response to other errors.

At a condition of steady state, with the gain parameter greater than critical, the steady state error in $z$ is zero. Because of this, the previously calculated values for steady state pitch angle, heave, and control deflection are still valid (Equations (174) through (177)). Moreover, because any controllable disturbance will result in a steady state condition these values apply for cases where the gain parameter is less than critical.

For conditions where the gain parameter is less than critical, the resulting control law is:

$$\delta = K_1 w + K_2 q + K_3 \theta + K_4 z + \eta K_s sign(\sigma) \tag{198}$$

And the steady state value of z is:

$$z_{ss} = \frac{\delta_{ss} - K_1 w_{ss} - K_3 \theta_{ss} - \eta K_s sign(\sigma)}{K_4} \tag{199}$$

Expressed in linear state space form for control law design, the representation for the SUBOFF at six knots is:

$$\begin{bmatrix} \dot{w} \\ \dot{q} \\ \dot{\theta} \\ \dot{z} \\ \dot{z}_I \end{bmatrix} = \begin{bmatrix} -0.0179 & 3.7101 & 0.0196 & 0 & 0 \\ 0.0006 & -0.068 & -0.0034 & 0 & 0 \\ 0 & 1 & 0 & 0 & 0 \\ 1 & 0 & -10.1269 & 0 & 0 \\ 0 & 0 & 0 & 1 & 0 \end{bmatrix} \begin{bmatrix} w \\ q \\ \theta \\ z \\ z_I \end{bmatrix} + \begin{bmatrix} -0.1009 \\ -0.0027 \\ 0 \\ 0 \\ 0 \end{bmatrix} \delta + \begin{bmatrix} F_d \\ M_d \\ 0 \\ 0 \\ 0 \end{bmatrix} \tag{200}$$

Utkin's method was applied to obtain a suitable control law. After some experimentation, the diagonal of the minimization matrix Q was selected as $Q_{11} = 100$, $Q_{22} = 100$, $Q_{33} = 100$, $Q_{44} = 1$, $Q_{55} = 0.01$. This yielded the following control law:

$$\sigma = 1.0w - 49.8158q - 12.7725\theta + 0.1050z + 0.0035z_I \tag{201}$$

$$\delta = -1.6009w + 161.0589q + 24.8125\theta - 0.0991z + K_s \eta satsign\left(\frac{\sigma}{\phi}\right) \tag{202}$$

$$|\delta| \leq 0.4 \tag{203}$$

Simulations of the SUBOFF under sliding mode integral control with a moment disturbance are given in Figure 32. For this state space system, control law, and disturbance set the value of $\eta_{crit}$ was (0.0484). Shown are five different values the ratio of the gain parameter to the critical gain parameter. For values of the ratio larger than about two, the system exhibited excessive oscillation before settling to zero depth error.

Simulations of the SUBOFF under sliding mode integral control with a force disturbance are given in Figure 33. For this state space system, control law, and disturbance set the value of $\eta_{crit}$ was (0.0466). Shown are six different values the ratio of the gain parameter to the critical gain parameter. For values of the ratio larger than about two, the system exhibited excessive oscillation before settling to zero depth error.

***Sliding mode disturbance response conclusions***

Submarine vertical plane depth control using sliding mode control can be effectively achieved in the presence of disturbances. Sliding mode control is similar to linear state feedback in that the an external disturbance will result in a steady state depth error. However, if the gain parameters of the sliding mode control are not properly selected, a loss of depth control can occur.

Steady state error can be dealt with using feedforward or integral control. Integral control has several advantages. Application of integral control does not require knowledge of the disturbance. However, if the gain parameter is too small, windup of the integral term occurs. If the gain parameter is too large, excessive oscillations can be

introduced. The greatest advantage of integral control demonstrated was that gain parameters less than critical did not result in loss of depth stability.

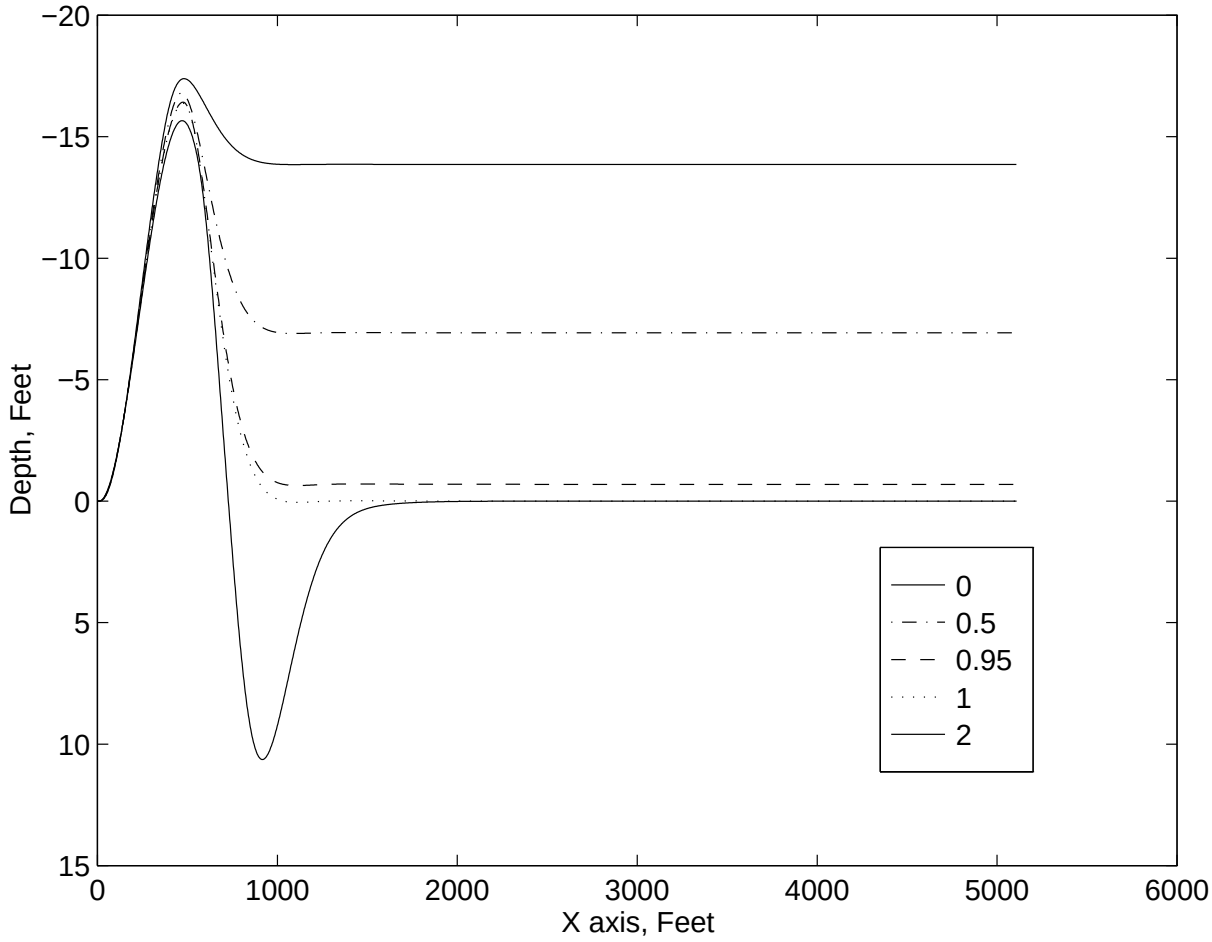


Figure 32. Nonlinear simulation of moment disturbance using sliding mode integral control

Feedforward control exhibited good disturbance compensation, assuming that the disturbances were measurable. Given the disturbances, feedforward values can be determined based upon the nonlinear equations of motion, requiring periodic nonlinear root finding, or upon the linear solution. Because of the computational expense of obtaining the nonlinear solution and the expected error in the hydrodynamic coefficients, a linear steady state solution is appropriate for feedforward computation.

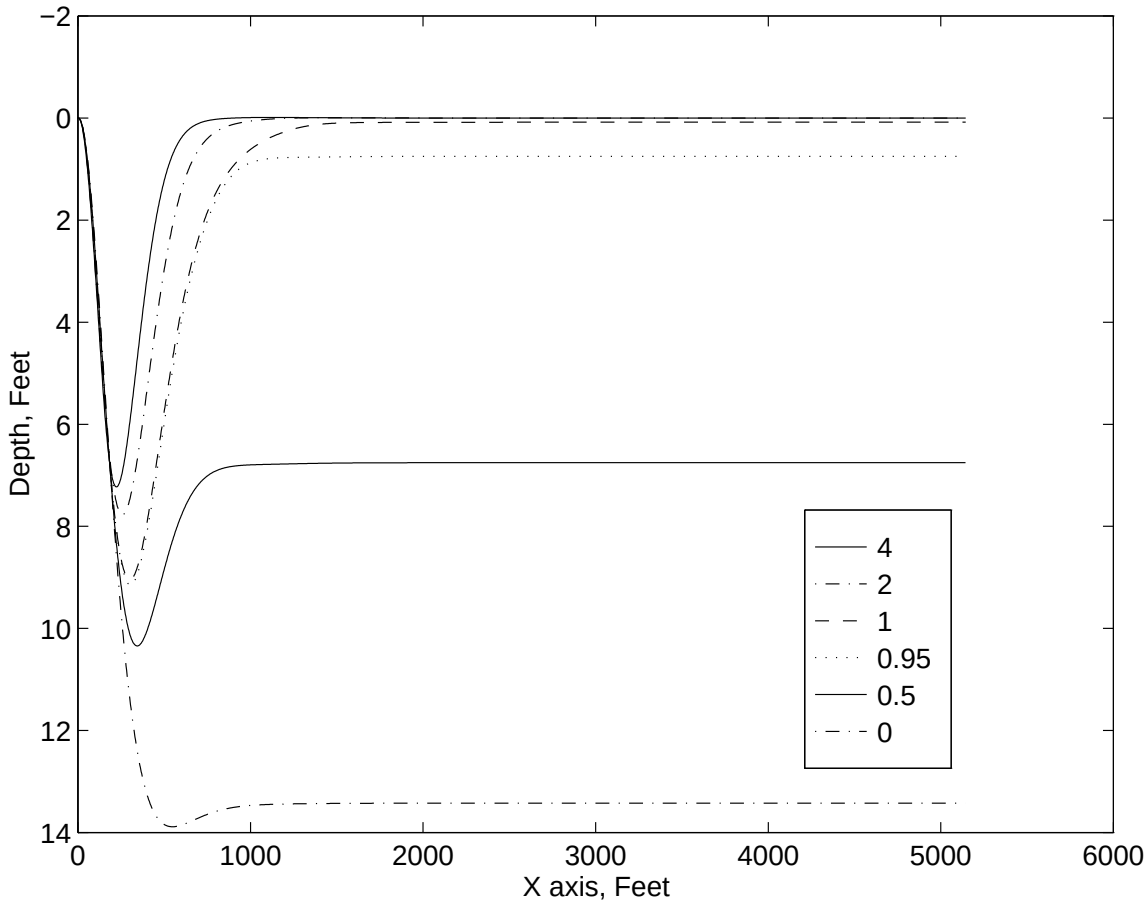


Figure 33. Nonlinear simulation of force disturbance using sliding mode integral control

## MIMO SLIDING MODE CONTROL AT PERISCOPE DEPTH

### Introduction

The purpose of using sliding mode control was to provide an alternate means of control which relied upon all the system states. The robust characteristics of sliding mode control were thought to be a good approximation to the human operators.

At periscope depth, experience dictates several desired conditions. First, the ship is trimmed heavy to counter the steady wave forces. Even more weight is brought on after this point to allow for a constant small positive trim angle, of several degrees. This provides reserve ballast which is made available by reducing the trim angle. Finally, in sea state three, it should be very possible to maintain depth within one foot of ordered depth.

The equations of motion used for this section are the nonlinear equations of submarine motion in the vertical plane. They are different from the equations used previously in this chapter, as they include both bow and stern planes. Also the force and moment disturbances used represent not only constant disturbances, like ships trim, but time varying wave forces as well. Repeated for convenience, the equations are:

$$\dot{w} = a_{11}uw + a_{12}uq + a_{13}\sin(\theta) + b_{11}u^2\delta_b + b_{12}u^2\delta_s + F_d\cos(\theta) + e_{11}q^2 + e_{12}qw \tag{204}$$

$$\dot{q} = a_{21}uw + a_{22}uq + a_{23}\sin(\theta) + b_{21}u^2\delta_b + b_{22}u^2\delta_s + M_d\cos(\theta) + e_{21}q^2 + e_{22}qw \tag{205}$$

$$\dot{\theta} = q \tag{206}$$

$$\dot{z} = w\cos(\theta) - u\sin(\theta) \tag{207}$$

$$\dot{x} = w\sin(\theta) + u\cos(\theta) \tag{208}$$

### Basic sliding mode controller

The sliding mode controller is of the same form as before, although with the introduction of MIMO control some of the scalar terms become vectors or matrices. The form of the basic sliding mode controller is:

$$\sigma_1 = S_{11}w + S_{12}q + S_{13}\theta + S_{14}\ z \tag{209}$$

$$\sigma_2 = S_{21}w + S_{22}q + S_{23}\theta + S_{24}\ z \tag{210}$$

$$\delta_b = K_{11}w + K_{12}q + K_{13}\theta + \eta_1 K_{s_{11}} satsign\left(\frac{\sigma_1}{\phi_1}\right) + \eta_2 K_{s_{12}} satsign\left(\frac{\sigma_2}{\phi_2}\right) \tag{211}$$

$$\delta_s = K_{21}w + K_{22}q + K_{23}\theta + \eta_1 K_{s_{21}} satsign\left(\frac{\sigma_1}{\phi_1}\right) + \eta_2 K_{s_{22}} satsign\left(\frac{\sigma_2}{\phi_2}\right) \tag{212}$$

$$|\delta_b| \le \delta_{\max} \tag{213}$$

$$|\delta_s| \le \delta_{\max} \tag{214}$$

As an initial attempt, Utkin's method was used to determine a sliding mode control law. After some experimentation, the diagonal of the minimization matrix Q was selected as $Q_{11} = 100$, $Q_{22} = 100$, $Q_{33} = 100$, $Q_{44} = 1$. This resulted in the following control matrices:

$$K = \begin{bmatrix} 39.6585 & -632.81 & -404.54 & 0 \\ -24.6916 & 429.65 & 250.27 & 0 \end{bmatrix} \tag{215}$$

$$S = \begin{bmatrix} 1 & 0 \\ 0 & 1 \\ -00985 & 1.7281 \\ 0.0170 & -0.0985 \end{bmatrix} \tag{216}$$

$$K_s = \begin{bmatrix} 10.9711 & -405.06 \\ 3.083 & 252.10 \end{bmatrix} \tag{217}$$

The values of the gain and boundary layer thickness parameters were taken as:

$$\eta_1 = \eta_2 = \frac{1}{20} \tag{218}$$

$$\phi_1 = \phi_2 = 1 \tag{219}$$

A SIMULINK® model was developed to incorporate the submarine dynamics of Chapter II, the wave forces of Chapter III, and the MIMO sliding mode control law. Also included was the trim model from Chapter IV.

The model was used to simulate a step change in commanded depth from 140 feet to 50 feet in depth. To provide some realism in the trim condition, the submarine was trimmed to 25 thousand pounds heavy, with no moment correction. Wave force values for sea state three were used, with a relative heading of 180 degrees (head seas). Figure 35 shows the resulting path taken by the submarine.

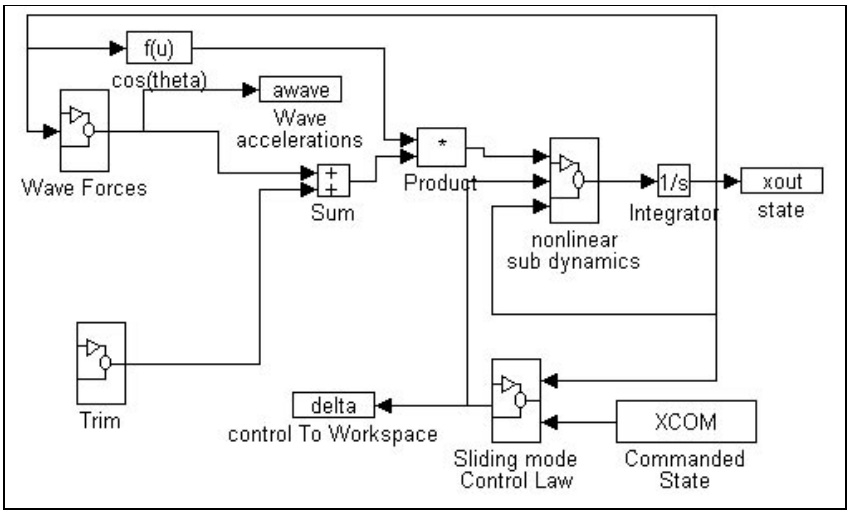


Figure 34. SIMULINK® model of submarine with wave forces and trim

At first glance, this control scheme fulfills most of the desired characteristics of a submarine depth controller. Periscope depth was achieved with no overshoot, and reasonable depth control was maintained. The trim condition was selected so that a steady state positive trim angle would exist at periscope depth. During the depth change, the maximum trim angle achieved was about ten degrees, which is also very consistent with actual submarine practice.

Inspection of Figure 36 shows some problems with this particular controller. The application of control effort was excessive. The main reason for this was the high frequency variations in $w$ and $q$ induced by the wave forces. Because of the combination of wave forces and trim, the commanded depth was not achieved. The average depth at periscope depth was 50.75 feet, as opposed to the commanded depth of 50 feet.

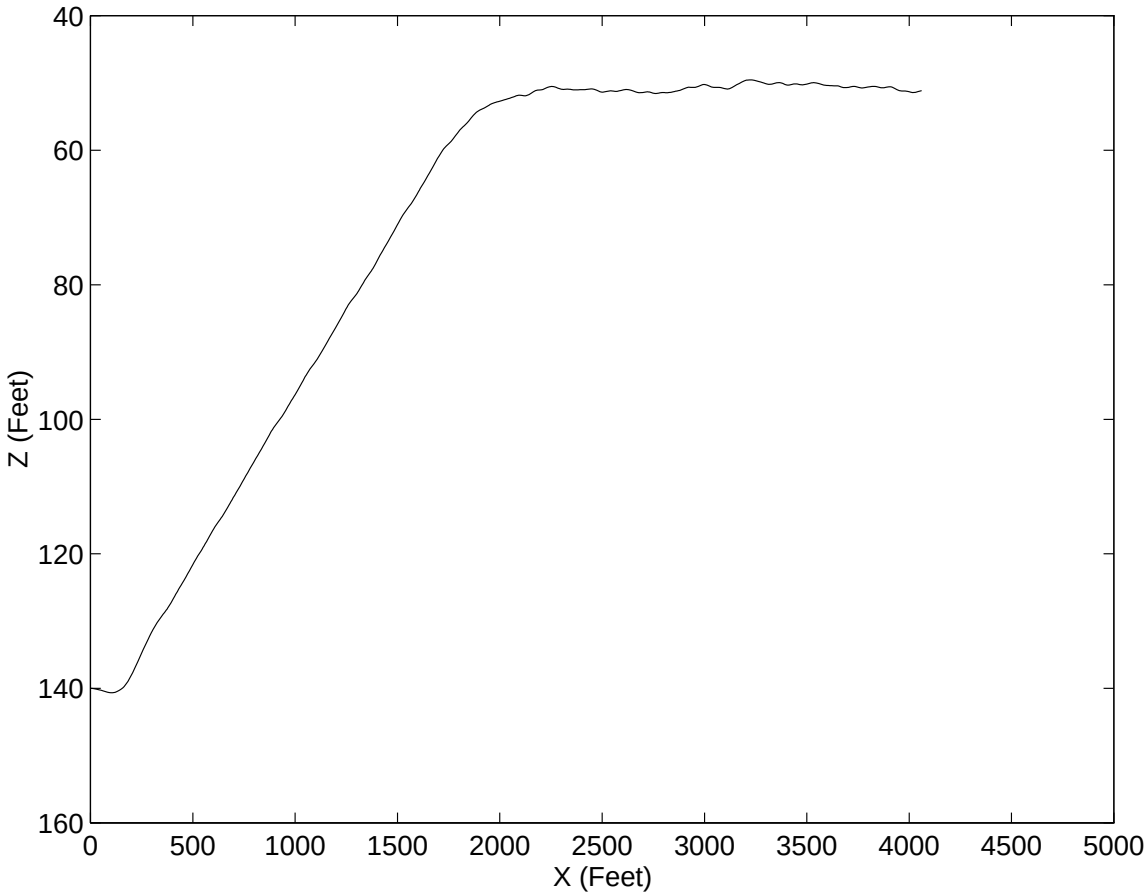


Figure 35. Basic sliding mode performance, step change approach to PD

Although the performance for the sea state three, head seas was adequate with this controller, it did not perform well with the other sea states or headings. Because of this, it was decided to use this control as a starting point for a performance optimization for each of the four sea state and direction cases available.

As was done for state feedback control, the MATLAB® CONSTR function was used to perform the optimizations. To provide a general set of design variables, the sliding mode linear quadratic regulator program was not used to determine the control law at each step of the optimization. Instead, the sliding surface itself was varied to change the control law.

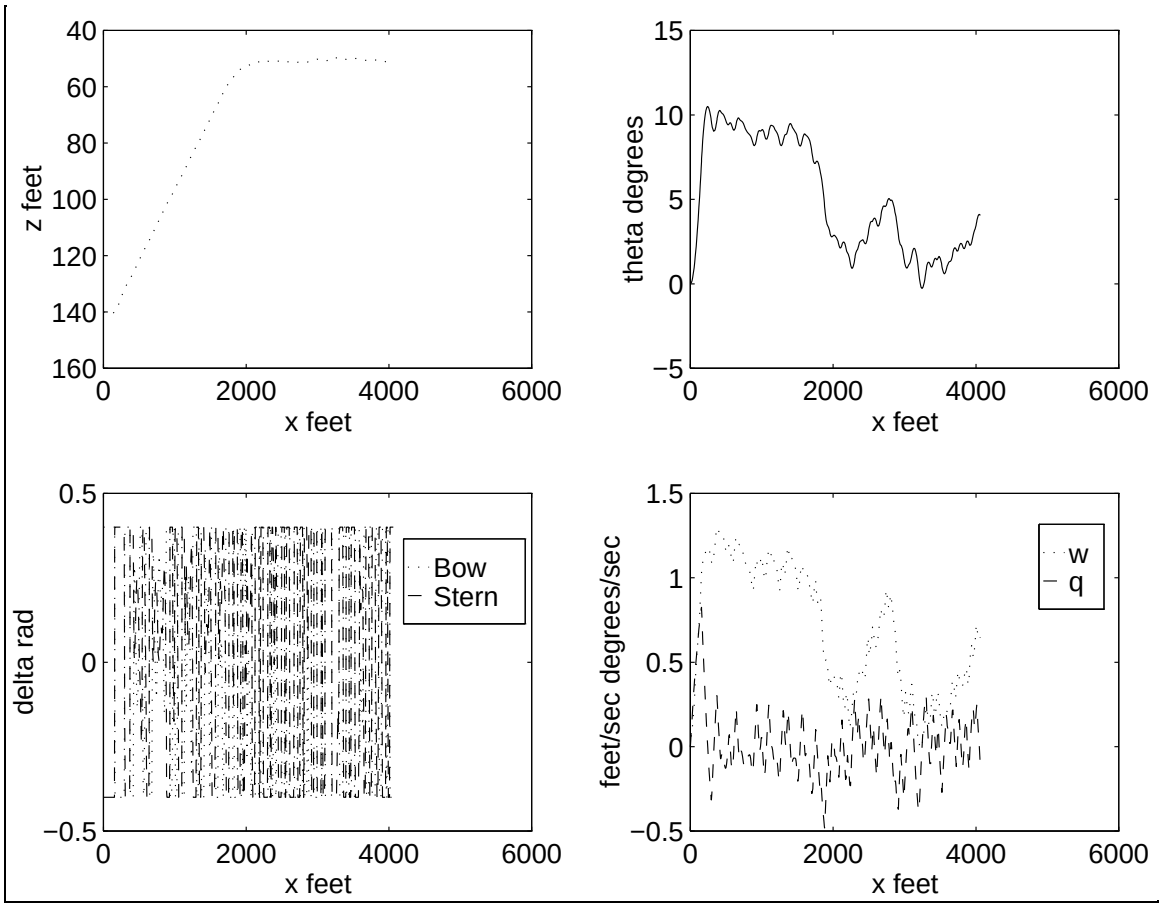


Figure 36. State parameters for basic sliding mode approach to periscope depth

The formal optimization statement is:

Minimize:

$$F(S_{31}, S_{32}, S_{41}, S_{42}, \eta_1, \eta_2, H, F) = \sqrt{\frac{\int_0^{t_f} (z - z_{mean})^2 \, dt}{t_f}} \tag{220}$$

where:

$z = depth$, determined by nonlinear simulation

$$z_{mean} = \frac{\int_0^{t_f} (z) dt}{t_f},$$

*H = Ballast added to center of buoyancy, thousands of pounds*

*F = Ballast shifted from forward to aft, thousands of pounds*

Subject to:

$$real(eigenvalues(A_{22} - A_{21}S_2^T)) \leq E_{\max} \tag{221}$$

Deviation from the mean value of depth vice the commanded was used because of the expected average depth error.

This approach was used for each of the four sea state cases. For sea state three (head

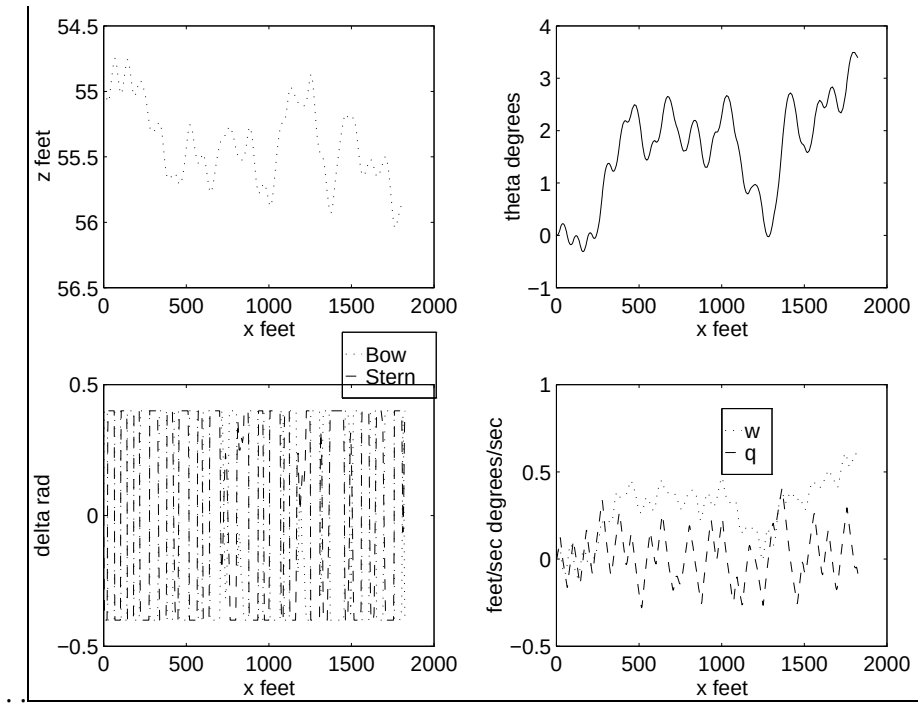


Figure 37. Simulation with basic sliding mode control in sea state three (head sea direction)

seas), the optimized response is shown in Figure 37. The results of the four optimizations are shown in Table 15. For the RMS error and maximum error, the optimized values are given, along with their percentage of the initial values. In all cases, use of the optimization resulted in reduction of the mean square depth error (measured from the average depth). Reduction of the maximum error was also achieved.

| **Sea State/Direction** | 3/head | | 3/beam | | 4/head | | 4/beam | |
|---|---|---|---|---|---|---|---|---|
| **Initial Values** | | | | | | | | |
| S | 1<br>0<br>-0.0985<br>0.0170 | 0<br>1<br>1.7281<br>-0.0985 | 1<br>0<br>-0.0985<br>0.0170 | 0<br>1<br>1.7281<br>-0.0985 | 1<br>0<br>-0.1388<br>0.0191 | 0<br>1<br>1.377<br>-0.694 | 1<br>0<br>-0.0932<br>0.0170 | 0<br>1<br>1.7281<br>-0.0903 |
| $K^T$ | 39.658<br>-632.81<br>-404.54<br>0 | -24.69<br>429.6<br>250.27<br>0 | 39.658<br>-632.81<br>-404.54<br>0 | -24.69<br>429.6<br>250.27<br>0 | 27.88<br>-491.0<br>-285.23<br>0 | -17.34<br>341.0<br>175.8<br>0 | 36.32<br>-632.77<br>-370.71<br>0 | -22.61<br>429.7<br>229.21<br>0 |
| $\eta_1$ / $\eta_2$ | 0.05/0.05 | | 0.05/0.05 | | 0.05/0.05 | | 0.0445/0.0445 | |
| H/F ($10^3$ pounds) | 20/0 | | 20/0 | | 20/0 | | 20/0 | |
| Mean Depth (feet) | 53.46 | | 49.55 | | 52.83 | | 54.53 | |
| RMS Error (feet) | 1.48 | | 3.37 | | 1.63 | | 2.75 | |
| Maximum Error (feet) | 3.00 | | 8.03 | | 4.20 | | 9.78 | |
| Sliding surface eigenvalues | -0.8725 + 0.5063i<br>-0.8725 - 0.5063i | | -0.8725 + 0.5063i<br>-0.8725 - 0.5063i | | -0.6981 + 0.4820i<br>-0.6981 - 0.4820i | | -0.8726 + 0.4172i<br>-0.8726 - 0.4172i | |
| **Optimized Values** | | | | | | | | |
| S | 1<br>0<br>-0.0816<br>0.0205 | 0<br>1<br>1.7244<br>-0.1203 | 1<br>0<br>-0.0196<br>0.0037 | 0<br>1<br>1.884<br>-0.0208 | 1<br>0<br>-0.1525<br>0.0176 | 0<br>1<br>1.3761<br>-0.0759 | 1<br>0<br>-0.933<br>0.0170 | 0<br>1<br>1.7281<br>-0.0903 |
| $K^T$ | 48.50<br>-631.1<br>-494.0<br>0 | -30.16<br>428.78<br>305.61<br>0 | 8.008<br>-695.15<br>-84.01<br>0 | -5.124<br>469.2<br>52.11<br>0 | 30.475<br>-490.8<br>-311.5<br>0 | -18.97<br>340.74<br>192.3<br>0 | 36.322<br>-632.76<br>-370.75<br>0 | -22.615<br>429.67<br>229.24<br>0 |
| $\eta_1$ / $\eta_2$ | 0.0488/0.0510 | | 0.0457/0.0457 | | 0.0501/0.0501 | | 0.0446/0.0445 | |
| H/F ($10^3$ pounds) | 19.9/0 | | 19.6/0.0 | | 20.0/0 | | 20.0/0 | |
| Mean Depth (feet) | 55.44 | | 57.61 | | 55.53 | | 54.57 | |
| RMS Error (feet) | 0.27 (18%) | | 0.84 (25%) | | 0.683 (42%) | | 1.43 (52%) | |
| Maximum Error (feet) | 0.77 (26%) | | 2.36 (29%) | | 1.92 (46%) | | 4.14 (42%) | |
| Sliding surface eigenvalues | -0.8725 + 0.6945i<br>-0.8725 - 0.6945i | | -1.7649<br>-0.1229 | | -0.6968 + 0.5434i<br>-0.6968 - 0.5434i | | -0.8726 + 0.4173i<br>-0.8726 - 0.4173i | |

Table 15. Optimized basic sliding mode control law results and performance

**Disturbance feedforward**

The sliding mode control can be implemented with a disturbance feedforward to correct average depth error. This can be implemented inside or outside of the sliding surface. For this example, the disturbance feedforward was implemented inside the sliding surface calculation.

$$\sigma = S^T x + S_5 \tag{222}$$

Assuming that neither sliding surface is saturated, that control deflection is within limits, and using a linear analysis, the steady state value of the depth error can be written as a linear combination of the force and moment disturbances (Appendix B).

$$z_{ss} - z_{commanded} = C_1 F_d + C_2 M_d \tag{223}$$

To eliminate the depth error, it is necessary to apply the same amount of control effort that the steady state error provides within the sliding surface:

$$S_5 = (z_{ss} - z_{commanded}) \begin{bmatrix} S_{41} \\ S_{42} \end{bmatrix} \tag{224}$$

This results in the following control law:

$$\begin{bmatrix} \delta_{bp} \\ \delta_{sp} \end{bmatrix} = \begin{bmatrix} K_{11} & K_{12} & K_{13} & 0 \\ K_{21} & K_{22} & K_{23} & 0 \end{bmatrix} \begin{bmatrix} w - w_{commanded} \\ q - q_{commanded} \\ \theta - \theta_{commanded} \\ z - z_{commanded} \end{bmatrix} + \begin{bmatrix} K_{s_{11}} & K_{s_{12}} \\ K_{s_{21}} & K_{s_{22}} \end{bmatrix} \begin{bmatrix} \eta_1 satsign\left(\dfrac{\sigma_1}{\phi_1}\right) \\ \eta_2 satsign\left(\dfrac{\sigma_2}{\phi_2}\right) \end{bmatrix} \tag{225}$$

$$\begin{bmatrix} \sigma_1 \\ \sigma_2 \end{bmatrix} = \begin{bmatrix} 1 & 0 \\ 0 & 1 \\ S_{31} & S_{32} \\ S_{41} & S_{42} \end{bmatrix}^T \begin{bmatrix} w - w_{commanded} \\ q - q_{commanded} \\ \theta - \theta_{commanded} \\ z - z_{commanded} \end{bmatrix} + \begin{bmatrix} C_1 S_{41} & C_2 S_{41} \\ C_1 S_{42} & C_2 S_{42} \end{bmatrix} \begin{bmatrix} \hat{F}_d \\ \hat{M}_d \end{bmatrix} \tag{226}$$

$$|\delta| \le \delta_{\max} \tag{227}$$

where the force and moment disturbances are filtered.

The initial sliding surface and gains from the basic sliding mode control law was used as the starting point for optimization. The formal optimization statement is:

$$F(S_{31}, S_{32}, S_{41}, S_{42}, \omega_{co}, \eta_1, \eta_2, H, F) = \sqrt{\frac{\int_0^{t_f} (z - z_{commanded})^2 \, dt}{t_f}} \tag{228}$$

Subject to:

$$real(eigenvalues(A_{22} - A_{21} S_2^T)) \leq E_{\max} \tag{229}$$

This approach was used for each of the four sea state cases. For sea state three (head seas), the optimized response is shown in Figure 38. The results of the four optimizations are shown in Table 16. For the RMS error and maximum error, the optimized values are given, along with their percentage of the initial values.

| **Sea State/Direction** | 3/head | | 3/beam | | 4/head | | 4/beam | |
|---|---|---|---|---|---|---|---|---|
| **Initial Values** | | | | | | | | |
| S | 1<br>0<br>-0.0985<br>0.0170 | 0<br>1<br>1.7281<br>-0.0985 | 1<br>0<br>-0.0985<br>0.0170 | 0<br>1<br>1.7281<br>-0.0985 | 1<br>0<br>-0.0985<br>0.0170 | 0<br>1<br>1.7281<br>-0.0985 | 1<br>0<br>-0.0985<br>0.0170 | 0<br>1<br>1.7281<br>-0.0985 |
| $K^T$ | 39.658<br>-632.81<br>-404.54<br>0 | -24.69<br>429.6<br>250.27<br>0 | 39.658<br>-632.81<br>-404.54<br>0 | -24.69<br>429.6<br>250.27<br>0 | 39.658<br>-632.81<br>-404.54<br>0 | -24.69<br>429.6<br>250.27<br>0 | 39.658<br>-632.81<br>-404.54<br>0 | -24.69<br>429.6<br>250.27<br>0 |
| $\omega_{co}$ (radians/second) | 0.25 | | 0.25 | | 0.25 | | 0.25 | |
| $\eta_1 / \eta_2$ | 0.05/0.05 | | 0.05/0.05 | | 0.05/0.05 | | 0.05/0.05 | |
| H/F ($10^3$ pounds) | 20/0 | | 20/0 | | 20/0 | | 20/0 | |
| Mean Depth (feet) | 55.28 | | 54.99 | | 55.10 | | 53.41 | |
| RMS Error (feet) | 0.4181 | | 1.50 | | 1.01 | | 7.04 | |
| Maximum Error (feet) | 1.225 | | 3.85 | | 3.50 | | 18.75 | |
| Sliding surface eigenvalues | -0.8725 + 0.5063i<br>-0.8725 - 0.5063i | | -0.8725 + 0.5063i<br>-0.8725 - 0.5063i | | -0.8725 + 0.5063i<br>-0.8725 - 0.5063i | | -0.8725 + 0.5063i<br>-0.8725 - 0.5063i | |
| **Optimized Values** | | | | | | | | |
| S | 1<br>0<br>-0.0981<br>0.0166 | 0<br>1<br>1.7281<br>0.096 | 1<br>0<br>-0.1255<br>0.0400 | 0<br>1<br>2.1291<br>-0.0473 | 1<br>0<br>-1.9567<br>-0.0445 | 0<br>1<br>3.8086<br>-0.1476 | 1<br>0<br>-0.1167<br>-0.0155 | 0<br>1<br>1.8775<br>-0.0240 |
| $K^T$ | 38.67<br>-632.8<br>-394.5<br>0 | -24.08<br>429.65<br>244.1<br>0 | 19.16<br>-795.53<br>-196.91<br>0 | -11.70<br>530.65<br>118.74<br>0 | 58.9<br>-1496.0<br>-599.1<br>0 | -37.3<br>948.4<br>377.5<br>0 | 9.906<br>-693.54<br>-95.02<br>0 | -5.992<br>467.3<br>60.9<br>0 |
| $\omega_{co}$ (radians/second) | 0.25 | | 0.350 | | 0.267 | | 0.245 | |
| $\eta_1 / \eta_2$ | 0.05/0.05 | | 0.0542/0.0578 | | 0.1853/0.0544 | | 0.0596/0.0548 | |
| H/F ($10^3$ pounds) | 20/0 | | 20.2/-0.1 | | 20.7/1.3 | | 20.1/0.0 | |
| Mean Depth (feet) | 55.22 | | 55.47 | | 55.45 | | 2.00 | |
| RMS Error (feet) | 0.405 (97%) | | 1.22 (81%) | | 1.01 (100%) | | 1.99 (28%) | |
| Maximum Error (feet) | 1.36 (111%) | | 3.20 (83%) | | 2.52 (72%) | | 4.93 (26%) | |
| Sliding surface eigenvalues | -0.8723 + 0.4813i<br>-0.8723 - 0.4813i | | -1.8706<br>-0.2984 | | -3.4649<br>-0.2992 | | -1.7409<br>-0.1211 | |

Table 16. Optimized sliding mode control with disturbance feedforward results and performance

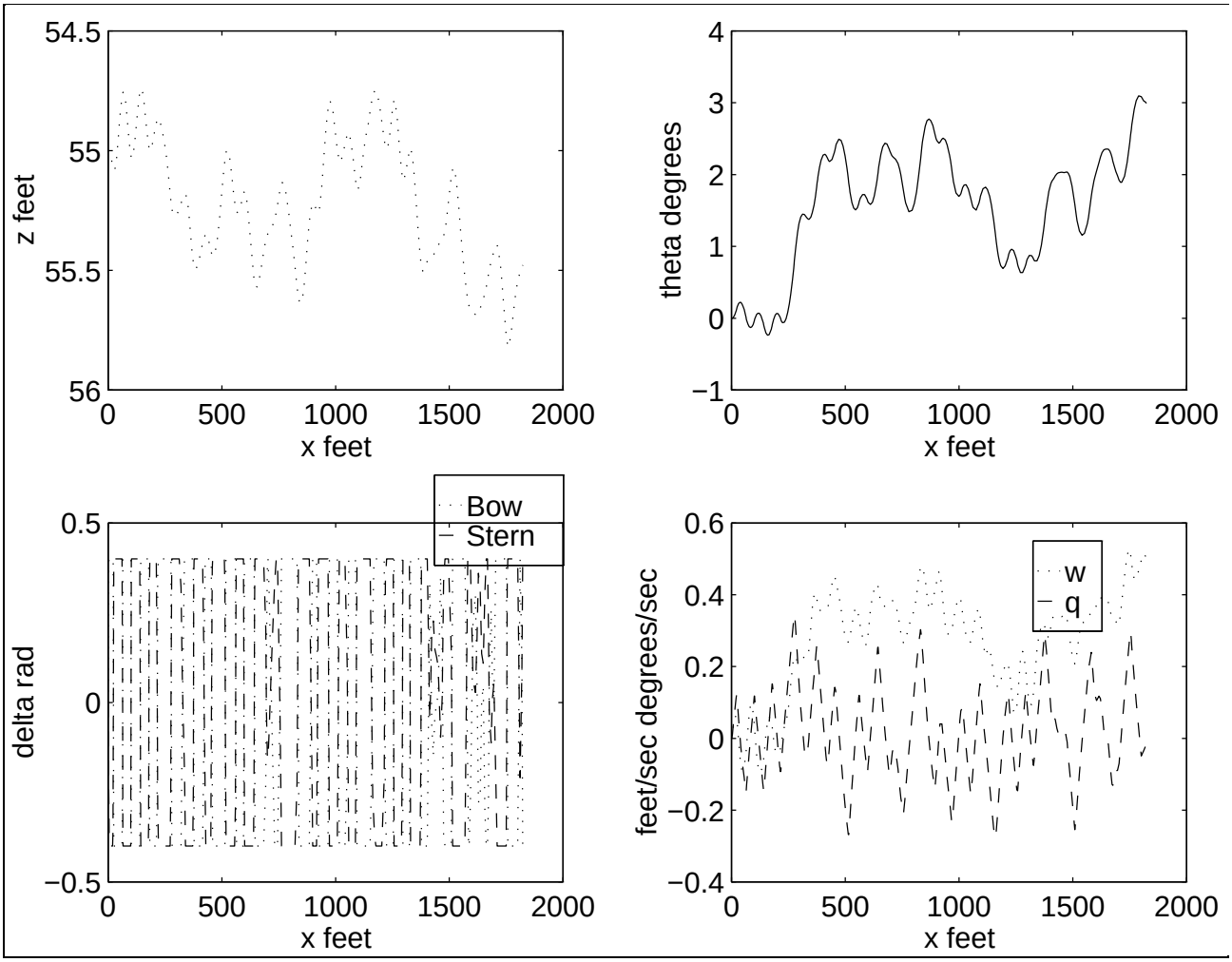


Figure 38. Simulation using sliding mode control with disturbance feedforward

**Integral control**

The sliding mode control law can be augmented with integral control on depth to remove the average depth error. This results in the following control law:

$$\begin{bmatrix}\delta_{bp}\\ \delta_{sp}\end{bmatrix}=\begin{bmatrix}K_{11} & K_{12} & K_{13} & K_{14} & 0\\ K_{21} & K_{22} & K_{23} & K_{24} & 0\end{bmatrix}\begin{bmatrix}w-w_{commanded}\\ q-q_{commanded}\\ \theta-\theta_{commanded}\\ z-z_{commanded}\\ z_I\end{bmatrix}+\begin{bmatrix}K_{s_{11}} & K_{s_{12}}\\ K_{s_{21}} & K_{s_{22}}\end{bmatrix}\begin{bmatrix}\eta_1 satsign\left(\dfrac{\sigma_1}{\phi_1}\right)\\ \eta_2 satsign\left(\dfrac{\sigma_2}{\phi_2}\right)\end{bmatrix} \tag{230}$$

$$\begin{bmatrix}\sigma_1\\ \sigma_2\end{bmatrix}=\begin{bmatrix}1 & 0\\ 0 & 1\\ S_{31} & S_{32}\\ S_{41} & S_{42}\\ S_{51} & S_{52}\end{bmatrix}^T\begin{bmatrix}w-w_{commanded}\\ q-q_{commanded}\\ \theta-\theta_{commanded}\\ z-z_{commanded}\\ z_I\end{bmatrix} \tag{231}$$

$$|\delta|\le\delta_{\max} \tag{232}$$

After a stable set of gains was determined, the controller was optimized to minimize the deviation from the commanded depth. The formal optimization statement is:

Minimize:

$$F(S_{31},S_{32},S_{41},S_{42},S_{51},S_{52},\eta_1,\eta_2,H,F)=\sqrt{\frac{\int_0^{t_f}(z-z_{commanded})^2\,dt}{t_f}} \tag{233}$$

Subject to:

$$real(eigenvalues(A_{22}-A_{21}S_2^T))\le E_{\max} \tag{234}$$

This approach was used for each of the four sea state cases. For sea state three (head seas), the optimized response is shown in Figure 39. The results of the four optimizations are shown in Table 17.

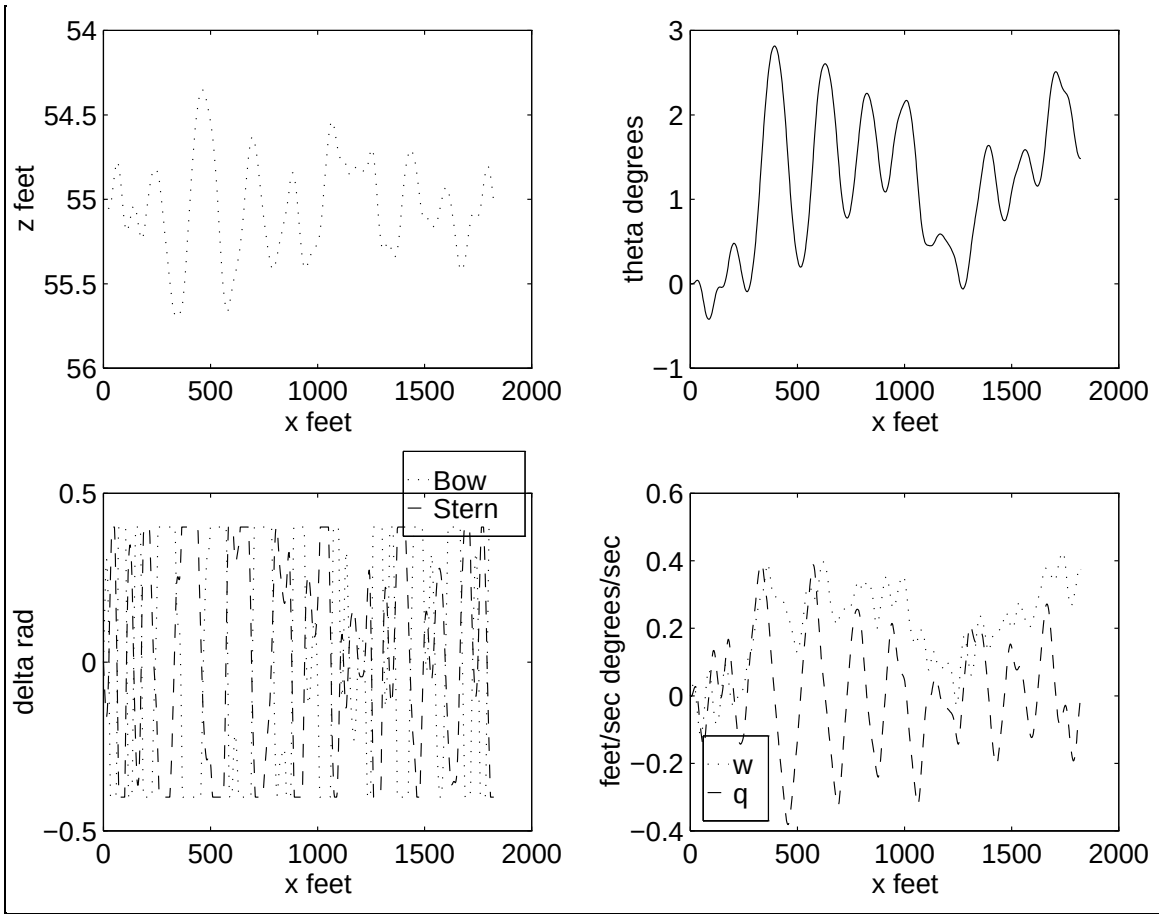


Figure 39. Simulation with sliding mode integral control in sea state three (head seas)

| **Sea State/Direction** | 3/head | | 3/beam | | 4/head | | 4/beam | |
|---|---|---|---|---|---|---|---|---|
| **Initial Values** | | | | | | | | |
| S | 1<br>0<br>-0.1038<br>0.0179<br>0.0005 | 0<br>1<br>1.7582<br>-0.1038<br>-0.0031 | 1<br>0<br>-0.1038<br>0.0179<br>0.0005 | 0<br>1<br>1.7582<br>-0.1038<br>-0.0031 | 1<br>0<br>-0.1038<br>0.0179<br>0.0005 | 0<br>1<br>1.7582<br>-0.1038<br>-0.0031 | 1<br>0<br>-0.1038<br>0.0179<br>0.0005 | 0<br>1<br>1.7582<br>-0.1038<br>-0.0031 |
| $K^T$ | 41.79<br>-645.08<br>-426.14<br>1.268<br>0 | -26.01<br>437.2<br>263.63<br>-0.7835<br>0 | 41.79<br>-645.08<br>-426.14<br>1.268<br>0 | -26.01<br>437.2<br>263.63<br>-0.7835<br>0 | 41.79<br>-645.08<br>-426.14<br>1.268<br>0 | -26.01<br>437.2<br>263.63<br>-0.7835<br>0 | 41.79<br>-645.08<br>-426.14<br>1.268<br>0 | -26.01<br>437.2<br>263.63<br>-0.7835<br>0 |
| $\eta_1$ / $\eta_2$ | 0.05/0.05 | | 0.05/0.05 | | 0.025/0.025 | | 0.05/0.05 | |
| H/F ($10^3$ pounds) | 20/0 | | 20/0 | | 20/0 | | 20/0 | |
| Mean Depth (feet) | 54.82 | | 54.80 | | 55.00 | | 54.73 | |
| RMS Error (feet) | 0.4671 | | 1.47 | | 0.707 | | 13.3 | |
| Maximum Error (feet) | 1.14 | | 4.23 | | 2.03 | | 31.62 | |
| Sliding surface eigenvalues | -0.8722 + 0.5063i<br>-0.8722 - 0.5063i<br>-0.0316 | | -0.8722 + 0.5063i<br>-0.8722 - 0.5063i<br>-0.0316 | | -0.8722 + 0.5063i<br>-0.8722 - 0.5063i<br>-0.0316 | | -0.8722 + 0.5063i<br>-0.8722 - 0.5063i<br>-0.0316 | |
| **Optimized Values** | | | | | | | | |
| S | 1<br>0<br>-0.0106<br>0.0195<br>0.0002 | 0<br>1<br>0.2485<br>-0.0202<br>-0.0010 | 1<br>0<br>-0.0233<br>0.0197<br>0.0001 | 0<br>1<br>0.5120<br>-0.0152<br>-0.0007 | 1<br>0<br>-0.0767<br>0.0118<br>0.0005 | 0<br>1<br>1.5995<br>-0.0766<br>-0.0031 | 1<br>0<br>-0.1428<br>0.0177<br>0.0003 | 0<br>1<br>3.7927<br>-0.0624<br>0.0006 |
| $K^T$ | 7.931<br>-32.52<br>-83.24<br>0.3965<br>0 | -4.920<br>56.91<br>50.04<br>-0.245<br>0 | 5.945<br>-139.4<br>-63.13<br>0.271<br>0 | -3.682<br>123.3<br>37.51<br>-0.1681<br>0 | 30.73<br>-580.47<br>-314.13<br>1.266<br>0 | -19.18<br>397.3<br>194.52<br>-0.783<br>0 | 25.0<br>-1469.6<br>-256.2<br>0.20<br>0 | -15.6<br>950.0<br>157.8<br>0.10<br>0 |
| $\eta_1$ / $\eta_2$ | 0.0468/0.0464 | | 0.0461/0.0453 | | 0.025/0.025 | | 0.0436/0.0553 | |
| H/F ($10^3$ pounds) | 19.6/-0.1 | | 19.6/0.0 | | 20.0/0.0 | | 19.4/-0.1 | |
| Mean Depth (feet) | 54.98 | | 55.01 | | 55.02 | | 55.16 | |
| RMS Error (feet) | 0.2345 (50%) | | 0.713 (49%) | | 0.693 (98%) | | 1.47 (11%) | |
| Maximum Error (feet) | 0.789 (69%) | | 1.90 (45%) | | 1.92 (95%) | | 4.15 (13%) | |
| Sliding surface eigenvalues | -0.1090 + 0.4314i<br>-0.1090 - 0.4314i<br>-0.0500 | | -0.2418 + 0.2871i<br>-0.2418 - 0.2871i<br>-0.0481 | | -0.7834 + 0.3260i<br>-0.7834 - 0.3260i<br>-0.0446 | | -3.6194<br>-0.1971<br>0.0061 | |

Table 17. Optimized sliding mode integral control law results and performance

## CONCLUDING REMARKS

A comparison between the quality of control achieved by sliding mode control could conclude that the sliding mode control was inferior to state feedback control. This comparison would, however, neglect the added benefits of sliding mode control. The robust character of sliding mode control with the ability to provide reliable control for submarine control given uncertain hydrodynamic coefficients has been demonstrated for the NPS autonomous underwater vehicle program (Hawkinson, 1990).

The sliding mode optimizations did not substantially reduce the control chatter and attendant high actuation rates. Variations of the sliding mode boundary thickness did not alleviate the chatter.

Table 18 gives a summary of the RMS error achieved by each of the sliding mode optimizations. For comparison, it also includes the full state feedback results from Chapter IV. Although these were larger than the corresponding full state feedback cases, the sliding mode control proved to be much more robust in response to step changes in commanded depth. The sliding surface eigenvalues exhibited much more damping than the corresponding cases of full state feedback control. Also, it seemed to provide a more realistic average pitch angle for periscope depth operations.

| **Sea State/Direction** | **3/Head** | **3/Beam** | **4/Head** | **4/Beam** |
|---|---|---|---|---|
| **Control Scheme** | | | | |
| Full State | 0.037 | 0.2638 | 0.2683 | 1.24 |
| Basic sliding mode | 0.27 | 0.84 | 0.683 | 1.43 |
| Full State with feedforward | 0.0928 | 0.4121 | 0.400 | 0.792 |
| Sliding mode with disturbance feedforward | 0.405 | 1.22 | 1.01 | 1.99 |
| Full State integral | 0.0414 | 0.372 | 0.536 | 1.96 |
| Sliding mode with integral control | 0.2345 | 0.713 | 0.693 | 1.47 |

Table 18. Optimized RMS error (feet) of sliding mode control and full state feedback